Published in final edited form as:
Neuroscience. 2011 August 25; 189: 384–396. doi:10.1016/j.neuroscience.2011.05.042.

ETHANOL ALTERS CALCIUM SIGNALING IN AXONAL GROWTH CONES

Stephanie J. Mah, Ph.D.,
Center for Neuropharmacology & Neuroscience, Albany Medical College (MC-136), 47 New Scotland Ave., Albany, NY 12208, Telephone: 518-262-6957, Fax: 518-262-6957

Mark W. Fleck, Ph.D., and
Center for Neuropharmacology & Neuroscience, Albany Medical College (MC-136), 47 New Scotland Ave., Albany, NY 12208, Telephone: 518-262-6536, Fax: 518-262-5799

Tara A. Lindsley, Ph.D.
Center for Neuropharmacology & Neuroscience, Albany Medical College (MC-136), 47 New Scotland Ave., Albany, NY 12208, Telephone: 518-262-5415, Fax: 518-262-5799

Stephanie J. Mah: ssuozzo1@gmail.com; Mark W. Fleck: fleckm@mail.amc.edu; Tara A. Lindsley: lindslt@mail.amc.edu

Abstract

Calcium (Ca^{2+}) channels are sensitive to ethanol and Ca^{2+} signaling is a critical regulator of axonal growth and guidance. Effects of acute and chronic exposure to ethanol (22, 43, or 87 mM) on voltage-gated Ca^{2+} channels (VGCCs) in whole cells, and KCl-induced Ca^{2+} transients in axonal growth cones, were examined using dissociated hippocampal cultures. Whole-cell patch-clamp analysis in neurons with newly-formed axons (Stage 3) revealed that rapidly inactivating, low-voltage activated (LVA) and non-inactivating, high-voltage activated (HVA) currents were both inhibited in a dose-dependent manner by acute ethanol, with relatively greater inhibition of HVA currents. When assessed by Fluo-4-AM imaging, baseline fluorescence and Ca^{2+} response to ethanol in Stage 3 neurons was similar compared to neurons without axons, but peak Ca^{2+} transient amplitudes in response to bath-applied KCl were greater in Stage 3 neurons and were decreased by acute ethanol. The amplitude of Ca^{2+} transients elicited specifically in axonal growth cones by focal application of KCl was also inhibited by acute exposure to moderate-to-high concentrations of ethanol (43 or 87 mM), whereas a lower concentration (22 mM) had no effect. When 43 or 87 mM ethanol was present continuously in the medium, KCl-evoked Ca^{2+} transient amplitudes were also reduced in growth cones. In contrast, Ca^{2+} transients were increased by continuous exposure to 22 mM ethanol. Visualization using a fluorescent dihydropyridine analog revealed that neurons continuously exposed to ethanol expressed increased amounts of L-type Ca^{2+} channels, with greater increases in axonal growth cones than cell bodies. Thus, acute ethanol reduces Ca^{2+} current and KCl-induced Ca^{2+} responses in whole cells and axonal growth cones, respectively, and chronic exposure is also generally inhibitory despite apparent up-regulation of L-type channel expression. These results are consistent with a role for altered growth cone Ca^{2+} signaling in abnormal neuromorphogenesis associated with fetal alcohol spectrum disorders.

Correspondence to: Tara A. Lindsley, lindslt@mail.amc.edu.

Keywords

ethanol; calcium channel; axonal growth cone; hippocampal culture

1.0 Introduction

Despite widespread public awareness that alcohol is damaging to the fetus, alcohol consumption during pregnancy is common, and 3% of pregnant women have alcohol use disorders and are unable to abstain from alcohol (CDC, 2009). Fetal alcohol spectrum disorders (FASD) are caused by maternal consumption of alcohol during pregnancy and affect an estimated 2–5% of children in the United States (May et al., 2009). FASD is characterized by persistent and disabling neurobehavioral deficits, some of which result from damage to the developing hippocampus (West et al., 1981; Berman and Hannigan, 2000; Hamilton et al., 2003; Zucca and Valenzuela, 2010). Histopathologic studies have consistently demonstrated that developmental exposure to ethanol decreases the complexity of hippocampal dendritic arbors and spine density, and disorganizes axon trajectories in the hippocampus and in other brain regions (Pentney and Miller, 1992; Lindsley, 2006). These effects are consistent with disrupted process outgrowth and guidance. However, the mechanisms by which exposure to ethanol in utero produces abnormal neuronal morphology and circuitry are incompletely understood.

Neuronal morphogenesis is greatly influenced by intracellular calcium (Ca^{2+}) concentration, which is tightly regulated by numerous Ca^{2+} conducting channels, Ca^{2+} pumps and Ca^{2+}-binding proteins (Berridge et al., 2003; Bolsover 2005; Zheng and Poo, 2007). Some of these Ca^{2+} signaling components are highly sensitive to ethanol. Extensive research indicates that the function of voltage-gated calcium channels (VGCCs) is altered in a variety of neural cell types by exposure to ethanol at intoxicating concentrations (10–50 mM) (Walter and Messing, 1999). Acute ethanol generally inhibits L-, N- and P/Q-type voltage-gated calcium channels by various mechanisms (Wang et al, 1994; Huang and McArdle, 1994; Solem et al., 1997), whereas chronic ethanol up-regulates channel density (Messing et al., 1986; Dolin et al., 1987; McMahon et al., 2000; Newton et al., 2005). However, few studies to date have explored ethanol effects on either the Ca^{2+} currents or VGCCs in immature neurons and, to our knowledge, none have investigated whether ethanol affects Ca^{2+} signaling in the specialized motile tip of growing axons, called the growth cone. This is important because the growth cone is a localized site for detecting extracellular growth-regulating cues that influence extension and retraction dynamics as axons navigate to synaptic targets, and Ca^{2+} plays a central role in these events (Henley and Poo, 2004; Gomez and Zheng, 2006). That growth cones are unique with regard to Ca^{2+} signaling is suggested by studies reporting differential Ca^{2+} responses in the cell body and growth cone in response to simultaneous application of extracellular cues (Nishiyama et al., 2003). We elected to begin our investigations of ethanol effects on growth cone Ca^{2+} signaling in developing neurons by focusing on VGCCs. Not only are VGCCs sensitive to ethanol, they are the major source of Ca^{2+} influx and are expressed early during development, including on growth cones (Gottmann and Lux, 1995). In addition, evidence indicates the effects of ethanol on VGCC function in neural cell lines may be altered upon stimulation with growth factors that induce neurite outgrowth (Mullikin-Kilpatrick and Triestman, 1995; Bergamashi et al., 1995).

We previously reported that ethanol present continuously in the medium of low-density rat hippocampal pyramidal neuron cultures dose-dependently inhibits dendritic development (Yanni and Lindsley, 2000; Lindsley et al., 2002) and delays initial axon outgrowth, but that the rate of axon growth increases overall due to a shorter distance retracted during pauses

between bursts of elongation (Lindsley et al., 2003). The axonal growth cones formed in these cultures express functional VGCCs as early as 12 hours after plating and undergo redistribution and changes in channel subtype expression during development (Blalock et al., 1999; Pravettoni et al., 2000; Obermair et al., 2004), closely mirroring expression patterns observed in the mouse hippocampus (Schlick et al., 2010). Therefore, the current study sought to first characterize the whole cell VGCC currents in these neurons, at a stage of development when newly formed axons are growing, and their response to acute ethanol. This was followed by experiments to assess effects of acute and chronic ethanol on depolarization-evoked Ca^{2+} transients, and on L-type channel expression specifically in axonal growth cones.

2.0 Experimental Procedures

2.1 Isolation and Primary Culture of Rat Hippocampal Neurons

Primary cultures of hippocampal pyramidal neurons were prepared from fetal Sprague-Dawley rats (Taconic Farms) on gestational day 19, as described by Kaech and Banker (2006). Briefly, hippocampi were dissected from the cerebral hemispheres, cleaned of meninges, then dissociated by treatment with trypsin (0.25% for 15 min at 37°C), and triturated with a fire-polished Pasteur pipette. The neurons were plated in Minimal Essential Medium with 10% heat-inactivated horse serum at a density of 5650 cells/cm^2 on glass coverslips precoated with poly-L-lysine. After neurons were allowed to adhere for 2–3 hrs, the coverslips were transferred into serum-free neuron maintenance medium (Minimal Essential Medium with N2-supplement (Invitrogen), 0.1 mM pyruvate, and 10 mM HEPES) that was conditioned for 2 days by rat cortical astrocyte cultures. All experiments were performed using neuronal cultures 18–30 hr after plating, when neurons are actively extending processes but before they develop synapses.

2.2 Chronic Ethanol Exposure

To study the effects of chronic exposure to ethanol on VGCC functions, 100% USP ethanol was added to the neuron maintenance medium to achieve a final concentration of 22, 43 or 87 mM, just prior to transfer of the neurons from the plating medium. These concentrations of ethanol are comparable to levels commonly achieved in the blood of chronic alcoholics (100 to 400 mg/dl) and correlated with increased risk of CNS damage to the fetus (Maier and West, 2001). Control cultures received no ethanol. Control and ethanol-treated cultures were maintained in modular incubator chambers at 36°C in 5% CO_2 saturated with water or water/ethanol at the target concentration in the medium, which attenuates evaporation of ethanol from the medium over time (Yanni and Lindsley, 2000).

2.3 Identification of Pyramidal Neurons

Only pyramidal neurons, which make up greater than 90% of the cells in these cultures, were selected for testing the effects of chronic or acute ethanol exposure on VGCC functions. The criteria used to distinguish pyramidal neurons from GABAergic interneurons and non-neuronal cells are based on criteria of Dotti et al., (1988) and were described previously in Clamp and Lindsley (1998). Briefly, pyramidal neurons undergo a stereotyped developmental progression; first, they extend a lamella that surrounds the soma (Stage 1), then 2–5 neurites extend to reach lengths of ≤ 20 μm (Stage 2), until about 12 hrs after plating one of these neurites grows rapidly and acquires distinct axonal characteristics (Stage 3). At 1–2 d in vitro, Stage 3 pyramidal neurons have a cell body diameter of 15–20 μm, 2–5 undifferentiated neurites, and a single axon with length greater than 40 μm. Nonpyramidal neurons have spindle-shaped cell bodies of 8–10 μm diameter and 2–3 short, thick processes. Nonneuronal cells are flattened, have poor phase contrast, and lack distinct processes.

2.4 Whole-Cell Recording

Whole-cell patch-clamp recordings from Stage 3 hippocampal pyramidal neurons were obtained 18–30 hr after plating in medium without ethanol. Voltage clamp recordings were performed at room temperature (20–22°C) using an Axopatch 200B amplifier. Current signals were filtered a 2kHz with an 8-pole Bessel filter, digitized at 5kHz and stored on a Macintosh PowerPC-G3 computer. Recording microelectrodes (TW150F; World Precision Instruments, Sarasota, FL) had resistances of 2–5 MΩ when filled with an internal solution containing (in mM): 135 CsCl, 10 CsF, 10 HEPES, 5 EGTA, 1 $MgCl_2$, 0.5 $CaCl_2$, pH 7.2, 295 mOsm. Neurons were superfused continuously at a rate of 1 ml/min with standard extracellular solution containing (in mM): 145 NaCl, 3 KCl, 5 HEPES, 10 $BaCl_2$, 10 4-AP, 8 TEA-Cl, 1 $MgCl_2$, 10 glucose, 1 μM tetrodotoxin and 0.1 mg/ml phenol red, pH 7.3, 300 mOsm. Offset potentials were nullified prior to on-cell seal formation, and drift was minimized by use of an agar bridge to a ground pellet in 1 M KCl. Only cells having < 80 pA holding current at −80 mV holding potential (Rm > 1 GΩ) stably throughout recording duration were used for analysis. Perfusion of control, ethanol- or drug-containing solutions was controlled using a multivalve solution exchange system as described previously (Fleck, 2002). Voltage-gated currents were tested at 10 sec intervals and changes were monitored to equilibrium. Alterations to these standard conditions are given in the text and figure legends.

Voltage-gated calcium channel currents were elicited by voltage steps from −80 to −20 mV, which included both transient low-voltage activated (LVA) and sustained high-voltage activated (HVA) currents, versus steps from −40 to −20 mV to inactivate the LVA currents in isolation. Preliminary experiments determined that a membrane holding potential (V_{hold}) −40 mV was sufficient to fully inactivate the LVA currents in Stage 3 neurons and the V_{hold} −80 mV was sufficient to fully de-inactivate the LVA currents. Activation profiles were examined by voltage steps from −80 mV to various test potentials between −100 to 100 mV. Activation profiles were also examined by recording currents during a voltage ramp from −100 to 100 mV over 0.5 sec. Current densities were calculated using the whole-cell capacitance measurements from the compensation circuitry of the amplifier. $NiCl_2$ was added dropwise to the bath with perfusion stopped to achieve a final concentration of 100 μM.

2.5 Whole Cell and Axonal Growth Cone Ca^{2+} Imaging

The effects of chronic or acute ethanol exposure on depolarization-induced calcium transients were assessed using standard, non-ratiometric methods, essentially as described for Fluo-3 imaging by Shitaka et al., 1996, but taking advantage of more rapid loading and superior brightness of Fluo-4. Briefly, 18–30 hr after plating, cells were washed three times with Krebs-Ringer buffer (in mM; 140 NaCl, 3 KCl, 1 $MgCl_2$, 2 $CaCl_2$, 10 HEPES, 10 glucose, at pH 7.4 and 295–305 mOsm), then loaded with 2 μm Fluo-4-AM (InVitrogen) for 15 min at room temperature and rinsed again three times with fresh Krebs-Ringer buffer. All wash solutions contained the same concentration of ethanol as the neuron maintenance medium. The coverslip with Fluo-4-loaded cells was mounted on the stage of a Zeiss LSM 510 META microscope system, maintained at room temperature, and imaged using the 488nm excitation of the argon laser with fluorescence signal capture between 500 and 550nm. Because Fluo-4 is used at a single excitation wavelength, changes in relative Ca^{2+} concentration within a region of interest (ROI) were calculated using Zeiss AIM software. The average fluorescence pixel intensity at a given time minus background fluorescence in the same size ROI positioned in a cell free region of the coverslip (F) was divided by pre-stimulus basal fluorescence (F_0) in the same region (F/F_0, in arbitrary units).

2.5.1 Comparing Neurons at Different Stages of Development—Calcium imaging of the cell body of neurons at different stages of development was performed using a 25×/

0.8N.A. PlanApo water immersion objective focused on coverslip fields with 6–10 neurons. First, we collected baseline images, then bath-applied control buffer or buffer with 87 mM ethanol, then evoked Ca^{2+} transients by bath application of 7 mM KCl (in mM; 7 KCl, 136 NaCl, 1 $MgCl_2$, 2 $CaCl_2$, 10 HEPES, 10 glucose, at pH 7.4 and 295–305 mOsm), with or without 87 mM ethanol. Images were collected for 1 min after each addition of reagent. Calcimycin (1 μg/ml, Molecular Probes, Eugene, OR) and EGTA were added sequentially after imaging to determine maximum fluorescence (F_{max}) and minimum fluorescence (F_{min}), respectively. The peak amplitude of the responses of control neurons to buffer followed by the addition of KCl, or to ethanol followed by KCl, was calculated as percent of maximal fluorescence in a 18×25 pixel ROI positioned in the soma (%F). About 60% of all cells displayed a KCl-induced Ca^{2+} transient increase of greater than 15% over baseline, and were therefore included in the analyses. Neurons without an axon (Stage 1 + Stage 2) were considered together and compared to Stage 3 neurons.

2.5.2 Chronic Ethanol and Growth Cone Response at Stage 3—Calcium transients were evoked in axonal growth cones of Stage 3 neurons by the focal application of 70 mM KCl solution (in mM; 70 KCl, 73 NaCl, 1 $MgCl_2$, 2 $CaCl_2$, 10 HEPES, 10 glucose, at pH 7.4 and 295–305 mOsm) via picospritzer-controlled ejection through a polished glass micropipette (8 p.s.i., internal diameter = 3 μm) positioned approximately 100 μm from the growth cone. Responses were visualized with a 63×/1.4 N.A. PlanApo oil immersion objective. Following collection of 10 baseline fluorescence images, whole-cell Ca^{2+} response elicited by a 500 msec pulse of 70 mM KCl was recorded to confirm cell responsiveness. To verify a graded Ca^{2+} response in the axonal growth cone, responses to sequential 500, 250 and 100 msec pulses of 70 mM KCl were recorded every 592 msec with a 2.7× zoom at the growth cone. Effects of acute addition of ethanol were assessed by imaging graded responses, first in control buffer at time 0, then again 30 sec and 5 min after replacement with buffer containing 0, 22, 43 or 87 mM ethanol. In some experiments, the order of pulses was reversed or buffer without KCl was ejected from the pipette. To assess possible photobleaching, the same pattern and timing of stimulation was also performed with control buffer. Ca^{2+} responses to the 500 and 250 msec pulses of KCl were quantified in an 18×25 pixel ROI positioned in the axonal growth cone, and %Fluorescence was calculated as described above. To be included in the analyses, fluorescence in the ROI had to return to baseline between evoked Ca^{2+} transients and the shape of the axon had to be stable throughout the imaging session. More than 90% of cells met these criteria.

2.5.3 Acute Ethanol and Growth Cone Response at Stage 3—Depolarization-evoked responses within the growth cone ROI were measured in control buffer (F_0; Peak fluorescence at t=0), then again in the same ROI 30 sec and 5 min after the addition of Krebs-Ringer containing 22–87 mM (F_t; Maximal fluorescence at t=30 sec or 5 min). Values were calculated as percent change in maximal fluorescence at t=0.

2.5.4 Statistical Analyses—The effects of chronic ethanol treatment were determined by ANOVA with posthoc comparison using Newman-Keuls test, and for acute ethanol experiments, by Newman-Keuls test of repeated measures for each growth cone before and after ethanol addition. A *p*-value of <0.05 was considered significant. All statistical analyses were performed using Statistica software (StatSoft, Tulsa, OK).

2.6 DM-Bodipy-DHP binding

DM-Bodipy-DHP, a dihydropyridine (DHP), L-type Ca^{2+} channel antagonist conjugated to the fluorophore BODIPY (4,4-difluoro-4-bora-3a,4a-diaza-s-indacene) (Molecular Probes) was bound to hippocampal neurons and visualized by confocal microscopy to assess the expression of L-type channels; their cellular distribution and relative abundance. We

followed methods described previously, with minor modifications (Shitaka et al., 1996). To limit intracellular accumulation of fluorophores, neurons on coverslips were incubated for 10 min in the dark at room temperature with 100 nM DM-Bodipy-DHP in Krebs-Ringer buffer. After incubation, the neurons were washed rapidly 2 times by immersion for 30 sec in ice-cold Krebs-Ringer buffer to remove unbound label, and all fluorescence measurements were carried out within 10 min. All dye and rinse solutions were made with ethanol concentrations equal to that of the maintenance medium of the neurons. Immediately after labeling, the coverslip was placed on the stage of a confocal laser-scanning microscope and the fluorescence was visualized with a 63× 1.4 NA oil immersion objective and excitation and emission filter wavelengths of 488 and 515 nm, respectively. To permit comparison of fluorescence intensity in parallel cultures from different treatment groups, the same filters and image settings were used for all images. Under these conditions, the fluorescence was stable and photobleaching was minimized. To confirm the specificity of L-type channel labeling, some coverslips were incubated simultaneously with 100 mM DM-Bodipy-DHP and 10 μM nifedipine. To estimate the fluorescence intensity in the soma and in axonal growth cones, these regions were traced and the mean intensity in arbitrary units for the horizontal optical slices (~5 at <2 μm intervals), minus background in a region the same size but placed over a cell free area of the field, was calculated using Zeiss AIM software. The experiment was replicated in three separate culture preparations with 2–4 coverslips for each treatment group. As similar results were obtained in separate experiments, the data were combined after recalculating each measurement as a percent of the mean control for each experiment, then analyzed by ANOVA with Newman-Keuls post hoc tests using Statistica software (StatSoft, Tulsa, OK).

3.0 Results

3.1 Effect of Axon Specification on KCl-evoked Calcium Responses

Hippocampal pyramidal neurons undergo a stereotyped elaboration of axons and dendrites, described as stages, which mimics their development in vivo (Dotti et al., 1988; Craig and Banker, 1994). The earliest of these stages are achieved within a few hours after plating; neurons first form a lamellipodia that encircles the cell soma (Stage 1) followed by formation of several short minor processes (Stage 2). Axon specification occurs within the next 12 hours when one minor process extends rapidly, becoming the axon (Stage 3). A number of studies have generally observed both LVA and HVA currents and differential development of VGCCs during initial neurite outgrowth in these cultures (Yarri et al., 1987; Toselli and Taglietti, 1992; Kortekaas and Wadman, 1997; Chameau et al., 1999; Pravettoni et al., 2000; Shin et al., 2008). Other studies indicated that differentiation state may affect how ethanol acts on VGCC function (Mullikin-Kilpatrick and Trestman, 1995; Bergamashi et al., 1995). We, therefore, sought to determine whether effects of acute ethanol on Ca^{2+} signaling differ with the stage of hippocampal neuron development and focused on the establishment of an axon as a key developmental event.

The effects of depolarization by KCl and acute ethanol on relative levels of Ca^{2+} in neurons before they initiate axon outgrowth (Stage 1–2) or after axon specification (Stage 3) were measured in Fluo-4-AM-loaded hippocampal neurons 18–30 h after plating. Results are summarized in Figure 1, showing the response of Stage 2 (Fig. 1A) and Stage 3 (Fig. 1B) neurons during recording of baseline fluorescence in control buffer, followed by addition of either 87 mM ethanol or buffer, then by addition of KCl. No significant differences were observed between the baseline percent fluorescence of cells imaged before or after the acute addition of 87 mM ethanol, regardless of whether they had extended axons. Both control neurons, and neurons acutely exposed to 87 mM ethanol, displayed KCl-induced Ca^{2+} responses that were significantly greater in Stage 3 neurons than in Stage 1–2 neurons. However, the peak amplitude of Ca^{2+} response to KCl was reduced in Stage 3 neurons

exposed to 87 mM ethanol before KCl stimulation compared to Stage 3 control neuron response to KCl. The remainder of our investigations focused on ethanol effects on KCl-induced Ca^{2+} responses in Stage 3 neurons.

3.2 Characterization of Calcium Currents in Stage 3 Hippocampal Neurons In Vitro

To investigate the presence of functional Ca^{2+} channel subtypes in Stage 3 hippocampal pyramidal neurons in culture during the first 18–30 h after plating, we measured voltage-activated Ba^{2+} currents (I_{Ba}), with 10 mM $BaCl_2$ replacing $CaCl_2$, using whole-cell patch-clamp recording techniques. Sodium channels were blocked by 1 μM tetrodotoxin, and the relative amplitudes of LVA and HVA currents were assessed when I_{Ba} were elicited by step depolarizations from V_{hold} −80 or −40 mV, respectively, to various membrane potentials (Fig. 2). Rapidly inactivating LVA Ca^{2+} currents could be elicited in neurons held at −80 mV or more negative holding potentials, which had an average peak of 97 ± 10 pA and decay time constant of 19.9 ± 1.2 msec to a sustained current of 35 ± 3.0% of the peak remaining after 90 msec. LVA current was eliminated at −40 mV holding potential, leaving mostly intact the larger non-inactivating HVA current (Fig 2A). When examined by 100 ms duration progressive voltage steps, I_{Ba} activation peaked around +5 mV with a pronounced shoulder between −20 and −40 mV. More informative was activation by 0.5 s voltage ramp over the same range, which isolated 2 distinct currents with peak activation voltages corresponding to the LVA and HVA activation profiles seen in the voltage step results (Fig. 2B). Here too, it was clear that HVA was the dominant whole-cell current, which is consistent with previous findings in hippocampal neurons (Yaari et al., 1987; Ozawa et al., 1989; Kortekaas and Wadman, 1997). Voltage ramp data from 52 Stage 3 neurons revealed LVA currents that were, on average, 42 ± 3 pA and peaked around −30 mV under control conditions; HVA currents were 234 ± 22 pA and peaked around +5 mV. The ratio of HVA/LVA current amplitudes ranged from 2.3 to 12.5 across the 52 cells.

In conjunction with the voltage ramp protocols used to separate the LVA and HVA currents, specific channel blockers were tested in a subset of cells to further identify the channel types contributing to I_{Ba} in Stage 3 neurons. Bath perfusion of 5 μM nifedipine eliminated 15.1% of LVA current and 45.5% of HVA current, compared to pre-drug control conditions, and reduced the HVA/LVA ratio by ~35% from 6.8 ± 0.7 to 4.4 ± 0.6 (n = 11 neurons). In other cells, 500 nM ω-conotoxin GVIA eliminated 26.0% of LVA current and 54.2% of HVA current, and reduced the HVA/LVA ratio by ~33% from 6.5 ± 0.8 to 4.4 ± 0.8 (n = 12 neurons). Notably, both the LVA and HVA currents were entirely blocked by 100 μM $NiCl_2$, which was used in subsequent experiments for leak subtractions to better resolve the isolated Ca^{2+} currents. Notably, the leak subtracted currents (Fig. 4) showed a substantial contribution by the HVA component at the peak of the LVA current, which accounted for nearly half the measured LVA amplitude. The relatively modest inhibition by nifedipine and ω-conotoxin GVIA of LVA currents is therefore entirely consistent with their selective inhibition of L-type and N-type channels, which predicts 23% and 27% inhibition, respectively.

3.3 Acute Ethanol Inhibits Whole-Cell Calcium Currents

To determine whether Ca^{2+} channel function is altered by acute exposure to ethanol, whole cell LVA and HVA Ba^{2+} currents of Stage 3 hippocampal neurons were monitored continuously before and after ethanol perfusion (Fig. 3). Rapidly inactivating LVA and non-inactivating HVA currents were elicited by voltage ramps from V_{hold} −80 mV or −40 mV, respectively. After a steady baseline was established, ethanol (22, 43 or 87 mM) was added by perfusion in the external solution. Current amplitude changes were then monitored to equilibrium, which was generally between 1–3 minutes. Analyses of the voltage ramp data showed a dose-related inhibition of LVA and HVA current amplitudes, but with relatively

greater inhibition of HVA currents (Fig. 3A–B). Results of IV ramp analyses of these whole-cell current are summarized in Figure 3C. Ethanol at a concentration of 22 mM, reduced the LVA and HVA current amplitudes to 87.1% and 82.5%, respectively, compared to control cells not perfused with ethanol. The HVA/LVA ratio was 4.22 ± 0.46, compared to 4.35 ± 0.43 for controls. Greater inhibition was observed after perfusion with 43 mM ethanol, which reduced LVA and HVA current amplitudes to 75.2% and 55.9% of controls, and the HVA/LVA ratio to 3.28 ± 0.36. Perfusion with 87 mM ethanol further reduced the LVA and HVA current amplitudes to 62.3% and 31.7% of controls, the HVA/LVA ratio to 2.09 ± 0.19. Importantly, these currents did not recover more than 20% of reduced amplitude after 10 min wash-off. The same result was obtained in comparing I_{Ba} current densities after normalizing by whole-cell capacitance as when raw I_{Ba} amplitudes were compared. Whole cell capacitance values for Stage 3 neurons 18–30 h after plating ranged from 7–10 pF. As with nifedipine and ω-conotoxin GVIA above, the relatively small inhibition of LVA currents by ethanol was consistent with a selective inhibition of L-type and N-type channels, which predicts 34% inhibition of the LVA peak if 87 mM ethanol inhibits only the HVA component (Fig. 4).

3.4 Acute Ethanol Inhibits Calcium Transients in Axonal Growth Cones

Having observed that acute ethanol inhibited whole cell Ca^{2+} currents, we next focused on assessing ethanol effects on growth cone Ca^{2+} signaling. The effect of acute exposure to ethanol on depolarization-evoked Ca^{2+} response in axonal growth cones was examined using confocal imaging of Stage 3 neurons loaded with Fluo-4-AM 18–30 h after plating. Intracellular Ca^{2+} responses in the axonal growth cones and distal axon were elicited by focal application of 70 mM KCl positioned near the growth cone with a picospritzer. Growth cone changes in Ca^{2+} were readily visualized as a rapid rise and slower decay to basal Ca^{2+} levels (Fig. 5A). Only Stage 3 neurons with axonal growth cones in which KCl pulses of varying duration (250 and 500 msec) yielded progressively larger (graded) responses were subsequently treated with ethanol, and more than 90% met this criterion. For each neuron, Ca^{2+} was quantified in a region of interest (ROI) in the palm of the growth cone (for example of ROI placement, see Fig. 5A, red oval), for pulses of KCl before the addition of ethanol (t=0) and for the same pulse series applied 30 sec and 5 min after the addition of ethanol. The maximal amplitude of the transients was reduced in a time- and dose-dependent manner after adding ethanol, but the graded response and return to baseline was not affected (Fig. 5B). Pulse ejection of buffer without KCl had no effect (data not shown).

To quantify the effects of acute ethanol exposure on Ca^{2+} response in the growth cone, the peak amplitude of Ca^{2+} transients in the ROI in response to the 500 msec pulse of KCl was calculated and plotted as percent of the peak amplitude in control neurons recorded within 20 sec after this depolarizing pulse (t=0) (Fig. 5C). Maximal amplitudes of KCl-evoked Ca^{2+} transients were significantly reduced when recorded 30 sec or 5 min after addition of 87 mM ethanol, by 15.2% and 32.7%, respectively. Significant reductions in the peak amplitude of Ca^{2+} transients were also observed after the addition of 43 mM ethanol. Calcium transients were not significantly affected by the acute addition of 22 mM ethanol. The addition of buffer alone during repeated stimulations showed no detectable shift in baseline, suggesting that photobleaching was negligible during the course of the experiment. Thus, acute ethanol inhibited depolarization-induced Ca^{2+} transients in axonal growth cones, with significant inhibition observed only at moderate to high concentrations of ethanol.

3.5 Effect of Chronic Ethanol on Calcium Responses in Axonal Growth Cones

Previously, we showed that continuous exposure to 43 or 87 mM ethanol in the medium, beginning shortly after plating, alters axon growth dynamics during early stages of hippocampal neuron development in culture (Lindsley et al., 2003), but has no significant

effect on neuron survival for up to 14 days in these cultures (Yanni et al., 2000). To determine whether the same exposure conditions that altered axon growth dynamics also alter Ca^{2+} responses in axonal growth cones, we compared KCl-induced Ca^{2+} responses in the growth cones of Stage 3 neurons in cultures maintained for 18–30 h in control medium or medium containing 22, 43, or 87 mM ethanol. As withdrawal from ethanol is known to elicit numerous rapid effects, the same concentrations of ethanol were present in buffers used throughout the protocol for imaging.

Results are plotted as percent of total fluorescence, calculated as the maximal KCl-evoked fluorescence after the 500 msec pulse minus pre-stimulus fluorescence, divided by the total fluorescence after the addition of calcimycin and EGTA (Fig. 6). In control neurons, the mean amplitude of KCl-evoked Ca^{2+} transients in the axonal growth cone was 57.9% of total fluorescence. The time-course of the response to KCl was not altered by ethanol compared to controls (data not shown). Continuous exposure to 43 or 87 mM ethanol in the medium significantly reduced the mean amplitude of Ca^{2+} transients in the growth cone, to 51.4% and 29.5% of total fluorescence, respectively. In contrast, when neurons developed in the presence of 22 mM ethanol, the mean amplitude of Ca^{2+} transients evoked by KCl in the growth cone was significantly increased compared to controls, to 65.8% of total fluorescence.

In summary, acute exposure and chronic exposure to 43 or 87 mM ethanol both reduced the mean amplitude of calcium transients in growth cones compared to controls. Along with whole cell current data, these results are consistent with ethanol reducing calcium channel function. However, our finding that chronic exposure to the lower concentration of 22 mM ethanol *increased* the amplitude of calcium transients in growth cones compared to controls, raises the possibility that a second, opposing effect of ethanol, namely increased channel expression. Long-term, chronic ethanol exposure reportedly up-regulates L- and N-type VGCC expression in a variety of neuronal cell types (Walter and Messing, 1999; Newton et al., 2005). We therefore reasoned that chronic exposure to 22 mM ethanol and higher may have up-regulated channel expression thereby increasing calcium transient amplitude, but that only the 43 and 87 mM ethanol sufficiently inhibited channel function to overcome the effects of increased channel expression, resulting in a net decrease in calcium transient amplitude we observed at the higher chronic ethanol concentrations. To test this, we compared growth cone responses of neurons chronically exposed to 22 mM ethanol when they remained in 22 mM ethanol to their response when ethanol concentration was acutely increased to 87 mM. We first measured the KCl-evoked Ca^{2+} response in the growth cones of neurons exposed continuously to 22 mM ethanol, then again after increasing the concentration of ethanol in the bath to 87 mM. The results were plotted as percent maximal amplitude of the KCl-induced Ca^{2+} transient in the growth cone ROI before increasing the ethanol concentration (Fig. 7). Calcium response in the growth cone was significantly reduced after bath application of 87 mM ethanol, by 12.4% when recorded 30 sec later, and by 26.6% when recorded 5 min later. The time-course of the response to KCl was not altered by ethanol compared to controls (data not shown). The same protocol for changing solutions was performed without increasing the 22 mM ethanol concentration, and this had no effect on growth cone Ca^{2+} responses (data not shown). These results are consistent with chronic ethanol exposure up-regulating calcium channels on axonal growth cones.

3.6 L-Type VGCCs are Up-Regulated in Axonal Growth Cones by Chronic Ethanol

Whether the significant increase in KCl-evoked Ca^{2+} response in axonal growth cones continuously exposed to 22 mM ethanol was attributable to up-regulation of L-type channels expression was directly assessed by labeling of L-type channels in living cells with DM-Bodipy-DHP fluorescence, a dihydropiridine Ca^{2+} antagonist conjugated to a fluorophore. Cellular regions with bound fluorescent label, including the soma and axonal growth cone,

were readily visualized by confocal microscopy (Fig. 8). As expected from previous reports (Shitaka et al., 1996; Pravettoni et al., 2000), DM-Bodipy-DHP fluorescence in control neurons was intense on the soma where L-type VDCCs are expressed at high density (Fig. 8A,B). The minor processes and axon shaft were less intensely labeled overall, but puncta of labeling were consistently observed especially along the distal axon shaft and axonal growth cone (Fig. 8C). When 10 μM nifedipine was added during the period of dye loading, the intensity of fluorescence over the soma and along neurites was dramatically reduced, and punctate labeling nearly abolished (Fig. 8 D–F). In contrast, the addition of 1μM ω-conotoxin GVIA during dye-loading had no effect on the pattern or intensity of fluorescence (data not shown). This indicates that DM-Bodipy-DHP recognizes L-type VDCCs on hippocampal neurons 18–30 h after plating, including their axonal growth cones.

When ethanol was present continuously in the culture medium, beginning shortly after plating, the intensity of DM-Bodipy-DHP labeling on the soma and axonal growth cone of Stage 3 neurons was increased dramatically compared with control neurons (Fig. 8 G–I). The pattern of fluorescence intensity, including the presence of punctate labeling, was not altered by ethanol treatment. Similar to control neurons, nifedipine present during dye loading of ethanol exposed neurons decreased all but trace amounts of fluorescence (not shown). Summary plots of DHP-binding fluorescence quantification show that the increase in relative fluorescence intensity was especially pronounced in the growth cone (Fig. 9A), where the mean intensity increased to 239% of control in neurons exposed to 22 mM ethanol, and to nearly 400% in neurons exposed to 87 mM ethanol. Increases in the soma were also observed, but were significantly greater than controls only in neurons exposed to 87 mM ethanol (Fig. 9B).

4.0 Discussion

Our results in dissociated hippocampal neurons reveal several novel effects of ethanol on Ca^{2+} signaling during early stages of differentiation. First, we show that whole cell Ca^{2+} currents are reduced by about 50% in Stage 3 neurons by acute exposure to intoxicating concentrations of ethanol, due to modulation of the HVA more than the LVA component. Second, we find that depolarization-induced Ca^{2+} responses in axonal growth cones are inhibited to a similar extent by acute exposure to ethanol. Third, we show that chronic exposure to ethanol also generally reduces depolarization-induced Ca^{2+} responses in growth cones, but does so despite a marked up-regulation of L-type channel expression. In all cases, these effects become more pronounced with increasing ethanol concentrations. Although much evidence indicates both the function and expression of VGCCs are modulated by ethanol in a variety of neural cell types (Walter and Messing, 1999; McMahon et al., 2000; Newton et al., 2005; Zucca and Valenzuela, 2010), this is the first to report that ethanol affects Ca^{2+} signaling and L-type Ca^{2+} channel expression specifically in axonal growth cones of immature neurons, in a model system in which effects of ethanol on morphogenesis and axon growth dynamics are well-characterized (Clamp and Lindsley, 1998; Yanni and Lindsley, 2000; Lindsley et al., 2002; Lindsley et al., 2003). As Ca^{2+} signaling is regarded as a critical modulator of differentiation and survival of developing neuronal cells, including process out growth and response to guidance factors (Henley and Poo, 2004; Gomez and Zheng, 2006), altered VGCC activity may play an important role in the mechanisms of ethanol disruption of neuromorphogenesis.

4.1. Calcium Currents and Stage-specific Effects of Ethanol

Hippocampal neurons in culture are commonly known to express at least two distinct calcium currents; a transient, LVA current (T-type) that is only active from a resting membrane potential (V_{rest}) below −60 mV, and a larger sustained HVA (L, N- and P/Q-type) current that is only slightly enhanced at very negative V_{rest} (Yarri et al., 1987; Toselli

and Taglietti, 1992; Kortekaas and Wadman, 1997; Chameau et al., 1999; Pravettoni et al., 2000; Shin et al., 2008). Here, whole-cell patch-clamp analyses of Stage 3 neurons under control conditions revealed predominantly HVA current and a smaller LVA current, indicating both currents are already expressed at this early stage of development. About half the HVA current was sensitive to L-type blocker nifedipine and half to N-type blocker ω-conotoxin GVIA, which is in general agreement with I_{Ba} and Fura-2 analyses of Stage 3 hippocampal neurons depolarized by KCl in the presence of nifedipine or ω-conotoxin (Pravettoni et al., 2000). Visualization of HA-tagged L-type channels (Obermair et al., 2004), indicates both of these channel types are expressed on the axonal growth cone as well as the neuronal cell body in these cultures. The predominance of the HVA component at early stages of development when neurites first form, has also been reported in dissociated embryonic hippocampal cultures similar to ours (Yarri et al., 1987; Chameau et al., 1999), and in acutely dissociated rat neonatal hippocampal pyramidal neurons (Thompson and Wong, 1991).

Our observations comparing the proportion of cells responsive to KCl before and after axon specification are in line with results of Fura-2 imaging studies that showed 33% of neurons had detectable KCl-induced increases in Ca^{2+} at 0.5 DIV (when most neurons are Stage 1–2), whereas 74% showed increases at 2 DIV (presumably Stages 1–3) (Shitaka et al., 1996), in good agreement with current observations that about 60% of all cells were responsive to KCl 18–30 hours after plating. When we assessed relative baseline Ca^{2+} by Fluo-4 imaging under control conditions, we found no difference between Stage 3 neurons and neurons at earlier stages of development, but as expected from previous reports (Shitaka et al., 1996), the peak amplitude of KCl-induced Ca^{2+} response was significantly higher in more mature neurons. Others have also observed no effect of acute ethanol on basal intracellular calcium in hippocampal neuron cultures (Webb et al., 1996), though increased basal calcium due to release from internal stores has been reported (Mironov and Hermann, 1996; Xiao et al., 2005).

We were especially interested in whether the effects of ethanol differed before and after axon specification, as some studies using cell lines have detected differences in sensitivity to ethanol effects on VGCCs in differentiated versus undifferentiated states (Bergamashi et al., 1995; Mullikin-Kilpatrick and Triestman, 1995). Our findings indicate that ethanol significantly inhibited the amplitude of KCl-induced Ca^{2+} transients only in Stage 3 neurons but not in neurons at earlier stages of development before axon specification (Stage 1 and 2). We previously showed that the morphoregulatory effects of ethanol are correlated with stage of development in hippocampal cultures, as delaying the addition of ethanol until most neurons are Stage 3 results in significantly shorter, less branched dendrites at Stage 5 than when ethanol is added at plating (Lindsley et al., 2002). Developmental changes in the expression and subcellular distribution of Ca^{2+} channels may contribute to such differences in the sensitivity and adaptive responses of developing neurons to ethanol.

4.2. Effects of Acute Ethanol Exposure

The effects of acute ethanol exposure on whole-cell VGCCs in hippocampal neurons at early stages of development have not been previously reported. Here, we show that acute ethanol inhibited both HVA and LVA whole-cell current amplitudes, with relatively greater inhibition of the predominating HVA currents. The HVA current had both nifedipine-sensitive (L-type) and conotoxin-sensitive (N-type) components, each accounting for about half of the HVA current. The LVA current was predominantly transient (T-type), but with a sustained component most likely reflecting the L-type $Ca_V1.3$ channel (Avery and Johnston, 1996; Xu and Lipscombe, 2001; Striessnig et al., 2006; Liebmann et al., 2007). It is likely that the relatively small effects of ethanol on the LVA current could be entirely explained by selective inhibition of the HVA, due to the overlapping voltage ranges (Fig. 4). However,

we cannot rule out additional effects of ethanol directly on the L-type $Ca_V1.3$ component of the LVA current. This effect could not be attributed to reduced cell size, as current density was not affected. Our results are in general agreement with reports that chronic ethanol exposure decreases VGCC function in dissociated whole brain from neonatal rats (Lee et al., 1996) and cerebellar slices from juvenile mice (Servais et al., 2007). Inhibition of L-type VGCCs by acute ethanol, at 22–87 mM concentrations tested in the current study, has also been documented in isolated nerve terminals of rat neurohypophysis in which it decreases open channel probability (Wang et al., 1994), and in NGF-differentiated PC-12 cells where it promotes steady-state inactivation (Mullikin-Kilpatrick and Treistman, 1995). Acute ethanol also inhibits N- and P/Q-type channels in differentiated PC-12 cells via a mechanism antagonized by PKA (Solem et al., 1997). Our results were consistent with these previous findings, as we did not observe any change in the voltage dependence of activation of HVA or LVA currents even after profound inhibition of the peak current amplitudes. Moreover, the slow onset and poor wash-off of ethanol effects most likely point to an indirect mechanism of action as others have suggested.

The initial Fluo-4-AM imaging experiments we re concerned with acute effects of ethanol on KCl-evoked Ca^{2+} transients specifically in axonal growth cones. Our results indicate that the amplitude of Ca^{+2} transients was inhibited by ethanol in a time-dependent manner, as longer time intervals after KCl application induced progressively larger decreases in Ca^{2+} transients compared to Ca^{2+} transients in controls over the same time interval. The inhibitory effect of ethanol was also dose-dependent, as 87 mM and 43 mM ethanol reduced peak amplitudes by about 35% and 20%, respectively, and 22 mM ethanol was not inhibitory.

4.3. Effects of Chronic Ethanol Exposure

Ca^{2+} imaging experiments focused on chronic effects of ethanol that were identical to conditions that altered axon growth dynamics in our previous experiments (Lindsley et al., 2003). Here, our results indicated that continuous exposure to moderate or high concentrations of ethanol in the medium also reduced the amplitude of Ca^{2+} transients in axonal growth cones depolarized by KCl, but continuous exposure to lower concentrations of ethanol increased their amplitude. A likely explanation for this somewhat unexpected result was provided by two additional experiments. First, our observation that Ca^{2+} response in growth cones of neurons chronically exposed to 22 mM ethanol could be inhibited by ethanol, provided the concentration was high enough, argues against an effect of chronic low dose ethanol that in some way prevented the inhibitory effect of ethanol on mechanisms of Ca^{2+} flux. An alternative possibility, that chronic low dose ethanol increased the expression of growth cone Ca^{2+} channels was consistent with results of DHP-binding fluorescence analyses showing increased L-type Ca^{2+} channel expression in neurons chronically exposed to 22 mM ethanol. Surprisingly, we also observed several fold increases in L-type channel expression at the higher concentrations of ethanol that inhibited KCl-induced Ca^{2+} transients. Competition with nifedipine displaced DHP, demonstrating specificity of the assay. DHP-binding channels are up-regulated by chronic ethanol, especially in growth cones, but despite this increased expression growth cone calcium response to KCl is significantly blunted. Thus, we believe that chronic ethanol inhibits VGCCs current amplitude in growth cones of newly formed axons in hippocampal neuron cultures, even as it up-regulates L-type channel expression. Up-regulation of VGCCs is a well-documented effect of chronic ethanol exposure in mature neurons and neural cell lines (Messing et al., 1986; Dolin et al., 1987; McMahon et al., 2000; Newton et al., 2005), but this is the first demonstration of a similar increase in growth cones.

4.4. Implications of the Current Findings

In addition to playing a role in ethanol effects on neuromorphogenesis, altered Ca^{2+} signaling in developing neurons may also contribute to stage-specific vulnerability to the cytotoxic effects of ethanol or withdrawal from ethanol. We previously showed that chronic exposure to ethanol followed by withdrawal triggered cell death in Stage 5, but not in Stage 3 hippocampal neurons (Lindsley and Clark, 2004). Withdrawal-induced changes in cell survival are especially interesting given the lack of effect on survival when ethanol is present continuously for 14 days. The mechanisms of ethanol withdrawal-induced hyperexcitability and neurotoxicity in the adult rat hippocampus may include increased expression of VGCC channels (Fadda and Rossetti, 1998; Walter and Messing, 1999), such as increases in L-type Ca^{2+} channel expression revealed in the current experiments.

Several reports argue for the importance of the source of Ca^{2+} in regulating axon growth and guidance. For example, Ca^{2+} influx through L-type channels inhibits axon growth in cortical cultures (Hutchins and Kalil, 2008), whereas Ca^{2+} release from intracellular stores promotes axon growth (Jacques-Fricke et al., 2006). Some evidence supports the idea that ethanol-induced changes in the release of Ca^{2+} from intracellular stores might contribute to abnormal Ca^{2+} signaling in neurons, though high concentrations of ethanol are required to observe this effect (Leslie et al., 1990). We did not test this possibility in the current study, however, work of others suggests that under control conditions Ca^{2+} stores are not a major contributor to KCl-induced Ca^{2+} responses in early stages of hippocampal neuron development in culture, as depletion by thapsigargin prior to KCl depolarization has a relatively small effect (Shitaka et al., 1996). Nevertheless, additional studies are needed to directly assess the potential contribution of release from intracellular channels on Ca^{2+}-storing organelles to ethanol effects on Ca^{2+} signaling in developing neurons.

In summary, the current results are consistent with disruption of Ca^{2+} homeostasis in this model, at least in Stage 3 neurons. Given evidence that Ca^{2+} channel subtypes change expression and cellular distribution over this time-course in culture (Blalock et al., 1999; Pravettoni et al., 2000; Obermair, 2004), much the way they change during development in vivo (Schlick et al., 2010), further studies aimed at determining the effects of ethanol on specific Ca^{2+} channel subtype expression, at earlier and later stages of neuronal development, may shed light on the molecular basis for stage-specific vulnerability to ethanol-induced neuronal damage. The mechanisms responsible for altered Ca^{2+} responses in growth cones are currently under investigation and, based on key studies in other model systems, might involve changes in the expression or subcellular distribution of specific channel subtypes and modification of these channels by kinase/phosphophatase activity (Mameli et al., 2005; Servais et al., 2007; Zucca and Valenzuela, 2010). It must be noted, however, that although these cultures are well-suited to visualizing cell biological effects of ethanol within subscribed cellular compartments, they have the disadvantage of being removed from potentially important factors in the intact environment of the developing brain. Therefore, confirmation of these findings in vivo should be an important goal of future studies.

Research Highlights

Stage 3 hippocampal pyramidal neurons display HVA and LVA Ca^{2+} currents

Acute ethanol inhibits whole-cell Ca^{2+} current amplitudes

Acute and chronic ethanol inhibits KCl-induced Ca^{2+} transients in axonal growth cones

Chronic ethanol up-regulates L-type Ca^{2+} channel expression on axonal growth cones

Abbreviations

Ca^{2+}	calcium
Cal	Calcimycin
Ethanol	EtOH
LVA	low-voltage activated
HVA	high-voltage activated
ROI	region of interest
F_{max}	maximum fluorescence
F_{min}	minimum fluorescence
F_0	peak fluorescence before stimulation
F_t	maximum fluorescence at given time after stimulation
VGCCs	voltage-gated calcium channels
I_{Ba}	barium current
FASD	fetal alcohol spectrum disorders
DIC	differential interference contrast
V_{hold}	membrane holding potential
V_{rest}	resting membrane potential

Acknowledgments

The authors wish to thank Elizabeth Ruggiero for expert technical assistance and Joseph Mazurkiewicz, Ph.D. for helpful discussions regarding quantitative live-cell imaging. This research was supported by NIAAA R01AA11416 (to TAL).

References

Avery RB, Johnston D. Multiple channel types contribute to the low-voltage-activated calcium current in hippocampal CA3 pyramidal neurons. J Neurosci. 1996; 16:5567–5582. [PubMed: 8795613]

Bergamaschi S, Battaini F, Trabucchi M, Parenti M, Lopez CM, Govoni S. Neuronal differentiation modifies the effect of ethanol exposure on voltage-dependent calcium channels in NG 108–15 cells. Alcohol. 1995; 12:497–503. [PubMed: 8590609]

Berman RF, Hannigan JH. Effects of prenatal alcohol exposure on the hippocampus: spatial behavior, electrophysiology, and neuroanatomy. Hippocampus. 2000; 10:94–110. [PubMed: 10706221]

Berridge MJ, Bootman MD, Roderick HL. Calcium Signaling: Dynamics, homeostasis and remodeling. Mol Cell Biol. 2003; 4:517–529.

Blalock EM, Porter NM, Landfield PW. Decreased G-protein-mediated regulation and shift in calcium channel types with age in hippocampal cultures. J Neurosci. 1999; 19:8674–8684. [PubMed: 10493768]

Bolsover SR. Calcium signaling in growth cone migration. Cell Calcium. 2005; 37:395–402. [PubMed: 15820386]

CDC [Centers for Disease Control and Prevention]. Alcohol use among pregnant and nonpregnant women of childbearing age – United States, 1991–2005. MMWR Morb Mortal Wkly Rep. 2009; 58:529–532. [PubMed: 19478721]

Chameau P, Lucas P, Melliti K, Bournaud R, Shimahara T. Development of multiple calcium channel types in cultured mouse hippocampal neurons. Neuroscience. 1999; 90:383–388. [PubMed: 10215143]

Clamp PA, Lindsley TA. Early events in the development of neuronal polarity in vitro are altered by ethanol. Alcohol: Clin Exp Res. 1998; 22:1277–1284. [PubMed: 9756043]

Craig AM, Banker G. Neuronal Polarity. Annu Rev Neurosci. 1994; 17:267–310. [PubMed: 8210176]

Dolin S, Little H, Hudspith M, Pagonis C, Littleton J. Increased dihydropyridine-sensitive calcium channels in rat brain may underlie ethanol physical dependence. Neuropharmacology. 1987; 26:275–279. [PubMed: 2438583]

Dotti CG, Sullivan CA, B anker GA. The establishment of polarity by hippocampal neurons in culture. J Neurosci. 1988; 8:1454–1468. [PubMed: 3282038]

Fadda F, Rossetti ZL. Chronic ethanol consumption: from neuroadaptation to neurodegeneration. Prog Neurobiol. 1998; 56:385–431. [PubMed: 9775400]

Fleck MW. Molecular actions of (S)-desmethylzopiclone (SEP-174559), an anxiolytic metabolite of zopiclone. J Pharmacol Exp Ther. 2002; 302:612–618. [PubMed: 12130723]

Gomez TM, Zheng JQ. The molecular basis for calcium-dependent axon pathfinding. Nat Rev Neurosci. 2006; 7:115–125. [PubMed: 16429121]

Gottmann K, Lux HD. Growth cone calcium ion channels: Properties, clustering, and functional roles. Perspect Dev Neurobiol. 1995; 2:371–377. [PubMed: 7757406]

Hamilton DA, Kodituwakku P, Sutherland RJ, Savage DD. Children with Fetal Alcohol Syndrome are impaired at place learning but not cued-navigation in a virtual Morris water task. Behav Brain Res. 2003; 143:85–94. [PubMed: 12842299]

Henley J, Poo MM. Guiding neuronal growth cones using Ca^{2+} signals. Trends Cell Biol. 2004; 14:320–330. [PubMed: 15183189]

Huang G-J, McArdle JJ. Role of the GTP-binding protein G_o in the suppressant effect of ethanol on voltage-activated calcium channels of murine sensory neurons. Alcohol Clin Exp Res. 1994; 18:608–615. [PubMed: 7943663]

Hutchins BI, Kalil K. Differential outgrowth of axons and their branches is regulated by localized calcium transients. J Neurosci. 2008; 28:143–153. [PubMed: 18171932]

Jacques-Fricke BT, Seow Y, Gottlieb PA, Sachs F, Gomez TM. Ca^{2+} influx through mechanosensitive channels inhibits neurite outgrowth in opposition to other influx pathways and release from intracellular stores. J Neurosci. 2006; 26:5656–5664. [PubMed: 16723522]

Kaech S, Banker G. Culturing hippocampal neurons. Nat Prot. 2006; 1:2406–2415.

Kortekaas P, Wadman WJ. Development of HVA and LVA calcium currents in pyramidal CA1 neurons in the hippocampus of the rat. Dev Brain Res. 2007; 101:139–147. [PubMed: 9263588]

Lee YH, Spuhler-Phillips K, Randall PK, Leslie SW. Effects of prenatal ethanol exposure on voltage-dependent calcium entry into neonatal whole brain-dissociated neurons. Alcohol Clin Exp Res. 1996; 20:921–928. [PubMed: 8865969]

Leslie SW, Brown LM, Dildy JE, Sims JS. Ethanol and neuronal calcium channels. Alcohol. 1990; 7:233–236. [PubMed: 2158790]

Liebmann L, Karst H, Sidiropoulou K, van Gemert, Meijer OC, Poirazi P, Joels M. Differential effects of corticosteron on the slow after hyperpolarization in basolateral amygdale and CA1 region: Possible role of calcium channel subunits. J Neurophysiol. 2008; 99:958–968. [PubMed: 18077660]

Lindsley, TA. Effects of ethanol on mechanisms regulating neuronal process outgrowth. In: Miller, MW., editor. Brain Development: Normal Processes, Alcohol, and Nicotine. New York: Oxford University Press; 2006. p. 230-244.

Lindsley TA, Clark S. Ethanol withdrawal influences survival and morphology of developing rat hippocampal neurons in vitro. Alcohol Clin Exp Res. 2004; 28:85–92. [PubMed: 14745305]

Lindsley TA, Comstock LL, Rising LJ. Morphologic and neurotoxic effects of ethanol vary with timing of exposure in vitro. Alcohol. 2002; 28:197–203. [PubMed: 12551761]

Lindsley TA, Kerlin AM, Rising LJ. Time-lapse analysis of ethanol effects on axon growth in vitro. Dev Brain Res. 2003; 147:191–199. [PubMed: 15068009]

Maier SE, West JR. Drinking patterns and alcohol-related birth defects. Alcohol Res & Health. 2001; 25:168–174. [PubMed: 11810954]

Mameli M, Zamudio PA, Carta M, Valenzuela CF. Developmentally regulated actions of alcohol on hippocampal glutamatergic transmission. J Neurosci. 2005; 25:8027–8036. [PubMed: 16135760]

May PA, Gossage JP, Kalberg WO, Robinson LK, Buckley D, Manning M, Hoyme HE. Prevalence and epidemiologic characteristics of FASD from various research methods with an emphasis on recent in-school studies. Dev Disabil Res Rev. 2009; 15:176–192. [PubMed: 19731384]

McMahon T, Andersen R, Metten P, Crabbe JC, Messing RO. Protein Kinase Cε mediates up-regulation of N-type calcium channels by ethanol. Mol Pharm. 2000; 57:53–59.

Messing RO, Carpenter CL, Diamond I, Greenberg DA. Ethanol regulates calcium channels in clonal neural cells. Proc Natl Acad Sci. 1986; 83:6213–6215. [PubMed: 2426713]

Mironov SL, Hermann A. Ethanol actions on the mechanisms of Ca^{2+} mobilization in rat hipopcampal cells are mediated by protein kinase C. Brain Res. 1996; 714:27–37. [PubMed: 8861606]

Mullikin-Kilpatrick D, Treistman SN. Inhibition of dihydropyridine-sensitive Ca^{2+} channels by ethanol in undifferentiated and nerve growth factor-treated PC12 cells: interaction with the inactivated state. J Pharmacol Exp Ther. 1995; 272:489–497. [PubMed: 7853161]

Newton PM, Tully K, McMahon T, Connolly J, Dadgar J, Treistman SN, Messing RO. Chronic ethanol exposure induces an N-type calcium channel splice variant with altered channel kinetics. FEBS Letters. 2005; 579:671–676. [PubMed: 15670827]

Nishiyama M, Hoshino A, Tsai L, Henley JR, Goshima Y, Tessier Lavigne M, Poo M-M. Cyclic AMP/GMP-dependent modulation of Ca^{2+} channels sets the polarity of nerve growth-cone turning. Nature. 2003; 423:990–995. [PubMed: 12827203]

Obermair GJ, Szabo Z, Bourinet E, Flucher BE. Differential targeting of the L-type Ca^{2+} channel α_{1C} ($Ca_V1.2$) to synaptic and extrasynaptic compartments in hippocampal neurons. Eur J Neurosci. 2004; 19:2109–2122. [PubMed: 15090038]

Ozawa S, Tsuzuki K, Iino M, Ogura A, Kudo Y. Three types of voltage-dependent calcium current in cultured rat hippocampal neurons. Brain Res. 1989; 495:329–336. [PubMed: 2548673]

Pentney, RJ.; Miller, MW. Effects of ethanol on neuronal morphologenesis. In: Miller, MW., editor. Development of the Central Nervous System: Effects of Alcohol and Opiates. New York: Wiley; 1992. p. 71-107.

Pravettoni E, Bacci A, Coco S, Forbicini P, Matteoli M, Verderio C. Different localizations and functions of L-type and N-type calcium channels during development of hippocampal neurons. Dev Biol. 2000; 227:581–594. [PubMed: 11071776]

Schlick B, Flucher BE, Obermair GJ. Voltage-activated calcium channel profiles in mouse brain and cultured hippocampal neurons. Neuroscience. 2010; 167:786–798. [PubMed: 20188150]

Servais L, Hourez R, Bearzatto B, Gall D, Schiffmann SN, Cheron G. Purkinje cell dysfunction and alteration of long-term synaptic plasticity in fetal alcohol syndrome. PNAS. 2007; 104:9858–9863. [PubMed: 17535929]

Shin M-C, Kim C-J, Min B-I, Ogawa S, Tanaka E, Akaike N. A selective T-type Ca^{2+} channel blocker R(−) efonidipine. Naunyn Schmeidebergs Arch Pharmacol. 2008; 377:411–421.

Shitaka Y, Matsuki N, Saito H, Katsuki H. Basic fibroblast growth factor increases functional L-type Ca^{2+} channels in fetal rat hippocampal neurons: Implications for neurite morphogenesis in vitro. J Neurosci. 1996; 16:6476–6489. [PubMed: 8815926]

Solem M, McMahon T, Messing RO. Protein kinase A regulates inhibition of N- and P/Q-type calcium channels by ethanol in PC12 cells. J Pharmacol Exp Ther. 1997; 282:1487–1495. [PubMed: 9316863]

Striessnig J, Koschak A, Sinnergger-Brauns MJ, Hetzenauer A, Nguyen NK, Busquet P, Pelster G, Singewald N. Role of voltage-gated L-type Ca^{2+} channel isoforms for brain function. Biochem Soc Trans. 2006; 34:903–909. [PubMed: 17052224]

Thompson SM, Wong RKS. Development of calcium current subtypes in isolated rat hippocampal pyramidal cells. J Physiology. 1991; 439:671–689.

Tosselli M, Taglietti V. Kinetic and pharmacological properties of high- and low-threshold calcium channels in primary cultures of rat hippocampal neurons. Pflugers Arch. 1992; 421:59–66. [PubMed: 1378588]

Walter HJ, Messing RO. Regulation of neuronal voltage-gated calcium channels by ethanol. Neurochem Int. 1999; 35:95–101. [PubMed: 10405992]

Wang X, Wang G, Lemos JR, Triestman SN. Ethanol directly modulates gating of a dihydropyridine-sensitive Ca^{2+} channel in neurohypophysial terminals. J Neurosci. 1994; 14:5453–5460. [PubMed: 7521910]

Webb B, Suarez SS, Heaton MB, Walker DW. Calcium homeostasis in cultured embryonic rat septohippocampal neurons is altered by ethanol and nerve growth factor before and during depolarization. Brain Res. 1996; 729:176–189. [PubMed: 8876986]

West JR, Hodges CA, Black AC Jr. Prenatal exposure to ethanol alters the organization of hippocampal mossy fibers in rats. Science. 1981; 211:957–959. [PubMed: 7466371]

Xiao, Z-m; Li, Li-j; Yu, S-z; Lu, Z-n; Li, C-y; Zheng, J-q. Effects of extracellular Ca^{2+} influx and intracellular Ca^{2+} release on ethanol-induced cytoplasmic Ca^{2+} overload in cultured superior cervical ganglion neurons. Neurosci Lett. 2005; 390:98–103. [PubMed: 16115728]

Xu W, Lipscombe D. Neuronal $Ca_V1.3\alpha_1$ L-type channels activate at relatively hyperpolarized membrane potentials and are incompletely inhibited by dihydropyridines. J Neurosci. 2001; 21:5944–5951. [PubMed: 11487617]

Yanni PA, Lindsley TA. Ethanol inhibits development of dendrites and synapses in rat hippocampal pyramidal neuron cultures. Dev Brain Res. 2000; 120:233–243. [PubMed: 10775775]

Yarri Y, Hamon B, Lux HD. Development of two types of calcium channels in cultured mammalian hippocampal neurons. Science. 1987; 235:680–682. [PubMed: 2433765]

Zheng JQ, Poo M-m. Calcium signaling in neuronal motility. Annu Rev Cell Dev Biol. 2007; 23:375–404. [PubMed: 17944572]

Zucca S, Valenzuela F. Low concentrations of alcohol inhibit BDNF-dependent GABAergic plasticity via L-type Ca^{2+} channel inhibition in developing CA3 hippocampal pyramidal neurons. J Neurosci. 2010; 30:6776–6781. [PubMed: 20463239]

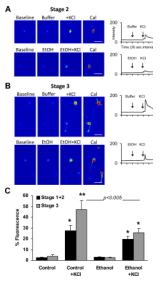

Figure 1. Effect of axon specification on intracellular calcium response to 7 mM KCl after acute exposure to 87 mM ethanol (EtOH) or buffer without ethanol

Hippocampal neurons were imaged 18–30 h after plating. Representative pseudocolor images of a Stage 2 (*A*) and Stage 3 (*B*) neuron and a corresponding plot of Fluo-4 fluorescence intensity (in arbitrary units) over time after addition of reagents (arrows). Images of peak fluorescence after addition of 1 ug/mL Calcimycin (Cal) under each condition are shown to better visualize cell morphology, but intensities are not plotted. For all treatment conditions, maximum and minimum fluorescence intensity was 233–245 and 1–10, after the addition of Cal and EGTA, respectively. *C*. Histogram plot of percent fluorescence values (calculated as described in Methods) in an 18×25 pixel region of interest (ROI) over the soma expressed as the means ± SEM. Data are the combined results of 3 separate cultures from which a total of 65 Stage 1 or Stage 2 neurons and 30 Stage 3 neurons were sampled from a total of 10 separate coverslips. **p* < 0.01 and ***p* < 0.001 compared to pre-stimulated values (repeated measures ANOVA with Dunnett post hoc test); *bar with p* < 0.005 compared Control + KCl response with Ethanol + KCl response (ANOVA with Newman-Keuls post hoc test). Scale bar = 50 μm

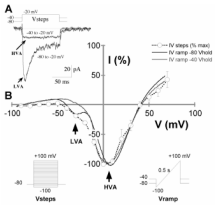

Figure 2. Whole-cell calcium currents in Stage 3 rat hippocampal pyramidal neurons

A. Representative I_{Ba} traces from Stage 3 neurons 18–30 h after plating. Currents were elicited by voltage steps to −20 mV from −80 or −40 mV holding potential. Rapidly inactivating, low-voltage activated (LVA) calcium currents were observed in neurons at holding potentials of −80 mV or more negative. Holding at −40 mV prior to the voltage ramp eliminated the LVA, leaving only the non-inactivating, high-voltage activated (HVA) current. *B.* Current-voltage plots showing the voltage-dependence of activation of LVA and HVA currents. Open circles are peak I_{Ba} amplitudes from voltage steps from −80 mV to various test potentials, interpolated by a dashed line. Solid lines are I_{Ba} amplitudes from voltage ramps preceded by holding potentials of −80 mV (black line) or −40 mV (gray line). Peak activation of LVA was −29.2 ± 0.9 mV. Peak activation of HVA was +5.6 ± 0.7 mV.

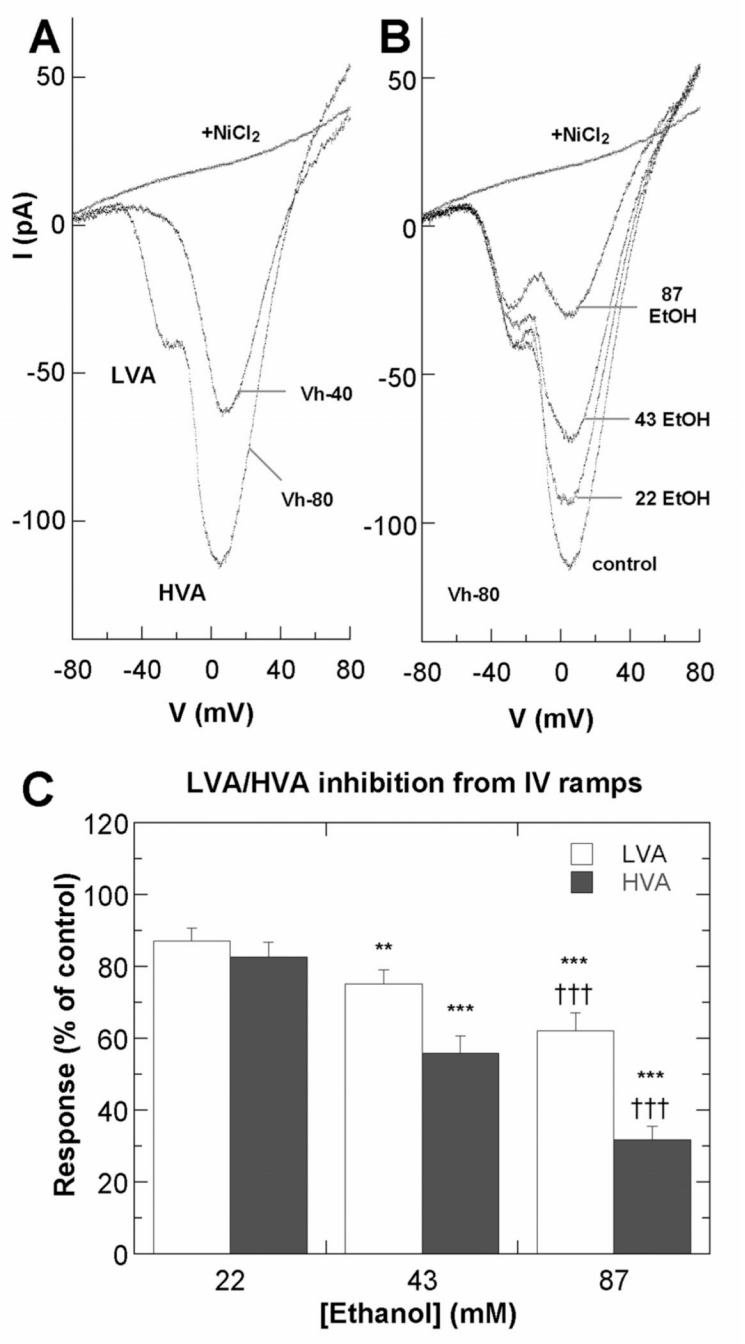

Figure 3. Ethanol inhibits VGCCs in hippocampal pyramidal neurons

A–B. Representative I_{Ba} currents from voltage ramps from Stage 3 neurons 18–30 h after plating. *A.* Current voltage properties of LVA and HVA currents in a control neuron at V_{hold} −40 or −80 mV before and after exposure to 100 μM $NiCl_2$. *B.* Current-voltage properties of LVA and HVA currents in an individual neuron at V_{hold} −80 mV before and after exposure to ethanol added by perfusion in the external solution. *C.* Summary of effects of ethanol on LVA and HVA currents, plotted as percent of peak amplitudes in the absence of ethanol. *Asterisk* indicates significant difference from the control group; *p < 0.005; **p < 0.0001 (n=15 neurons; repeated measures ANOVA with Dunnett posthoc test). *Cross* indicates significant difference from the 43 mM ethanol group; ††† p < 0.0001.

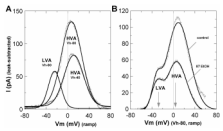

Figure 4. I_{Ba} components and ethanol inhibition after leak subtraction

A. Absolute values of LVA and HVA current components after subtraction of the $NiCl_2$-insensitive (leak) currents from voltage ramp data. Data from a representative Stage 3 neuron are shown as individual data points and fitted by one or two Gaussian distributions (solid lines). *B.* Leak-subtracted LVA and HVA current components in a representative neuron before and after exposure to 87 mM ethanol. In 6 cells compared before and after leak subtraction, inhibition of LVA current by 87 mM ethanol averaged 41% before and 30% after subtraction, whereas inhibition of HVA currents averaged 69% before and 61% after subtraction (not shown). Together, these results confirm greater sensitivity of HVA currents even though nearly half the measured peak of LVA current reflects the HVA component, and that ethanol effects are not related to altered leak currents.

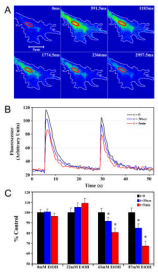

Figure 5. Acute ethanol inhibits depolarization-evoked calcium signals in axonal growth cones

A. Representative pseudocolor fluorescence images of a KCl-induced Ca^{2+} in the axonal growth cone of a hippocampal pyramidal neuron 24 h after plating. *B.* Traces of Ca^{2+} in a region of interest in the palm of the same growth cone, when evoked by KCl pulses of 500 msec (*left*) and 250 msec (*right*), before (t = 0; black line), and at 30 sec (blue line) and 5 min (red line) after bath application of 87 mM ethanol. Ethanol inhibition of the peak fluorescence intensity increases with time. Ethanol does not alter the graded response to pulse duration and Ca^{2+} returns to baseline between pulses. *C.* Histogram plot of peak amplitudes of KCl-evoked calcium transients in axonal growth cones before, and at 30 sec and 5 min after the addition of 22, 43 or 87 mM ethanol. Data are the mean ± SEM peak fluorescence expressed as a percent of control transients evoked by the 500 msec pulse. The inhibitory effect of ethanol is dose- and time-dependent. * $P < 0.01$, ** $P < 0.001$; repeated measures ANOVA with Newman-Keuls posthoc test.

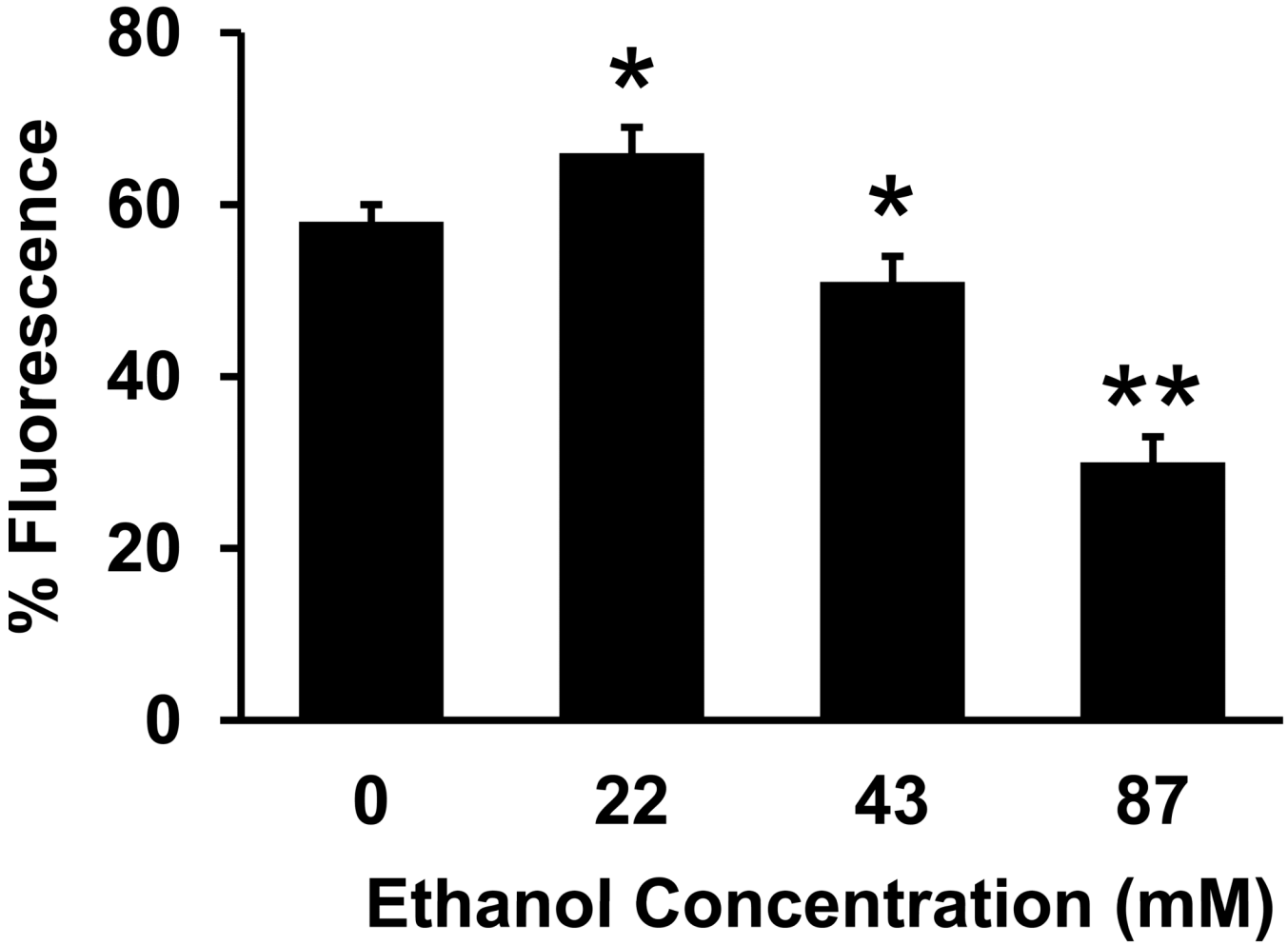

Figure 6. Continuous exposure to ethanol in the medium alters depolarization-evoked calcium transients in axonal growth cones

Plot of the mean peak fluorescence intensity in a ROI in the palm of the axonal growth cones of control neurons and of neurons maintained for 18–30 h in medium containing 22, 43 or 87 mM ethanol. Ethanol at 22 mM increases, and at 43 or 87 mM decreases KCl-induced Ca^{2+}20. Data are the mean ± SEM peak total fluorescence from 17–19 growth cones in each treatment group, collected from at least 3 separate cultures. * $P < 0.005$, ** $P < 0.0005$; ANOVA with Newman-Keuls posthoc test.

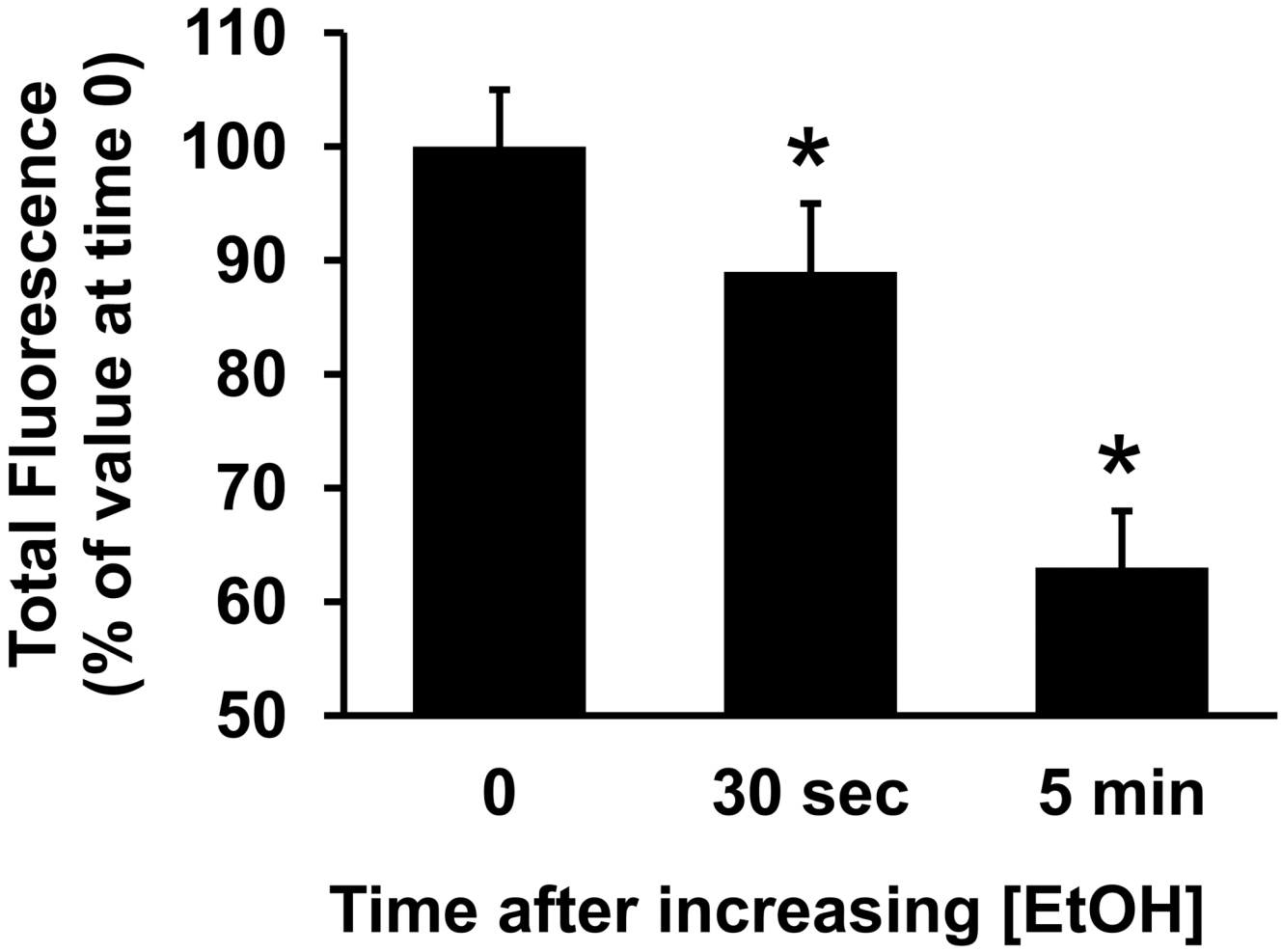

Figure 7. Interplay of acute and continuous ethanol exposure on calcium signaling in axonal growth cones

Plot of the mean peak fluorescence intensity of KCl-evoked calcium transients in a ROI in the palm of axonal growth cones of neurons maintained in medium containing 22 mM ethanol for 18–30 h, recorded before and at 30 sec and 5 min after increasing the concentration of ethanol in the bath to 87 mM ethanol. Data are the mean ± SEM peak fluorescence of 11 growth cones, expressed as a percent of transients evoked by the 500 msec pulse before increasing ethanol concentration. The inhibitory effect of ethanol is dose6 dependent. * $P < 0.05$, ** $P < 0.0005$; repeated measures ANOVA with Newman-Keuls posthoc test.

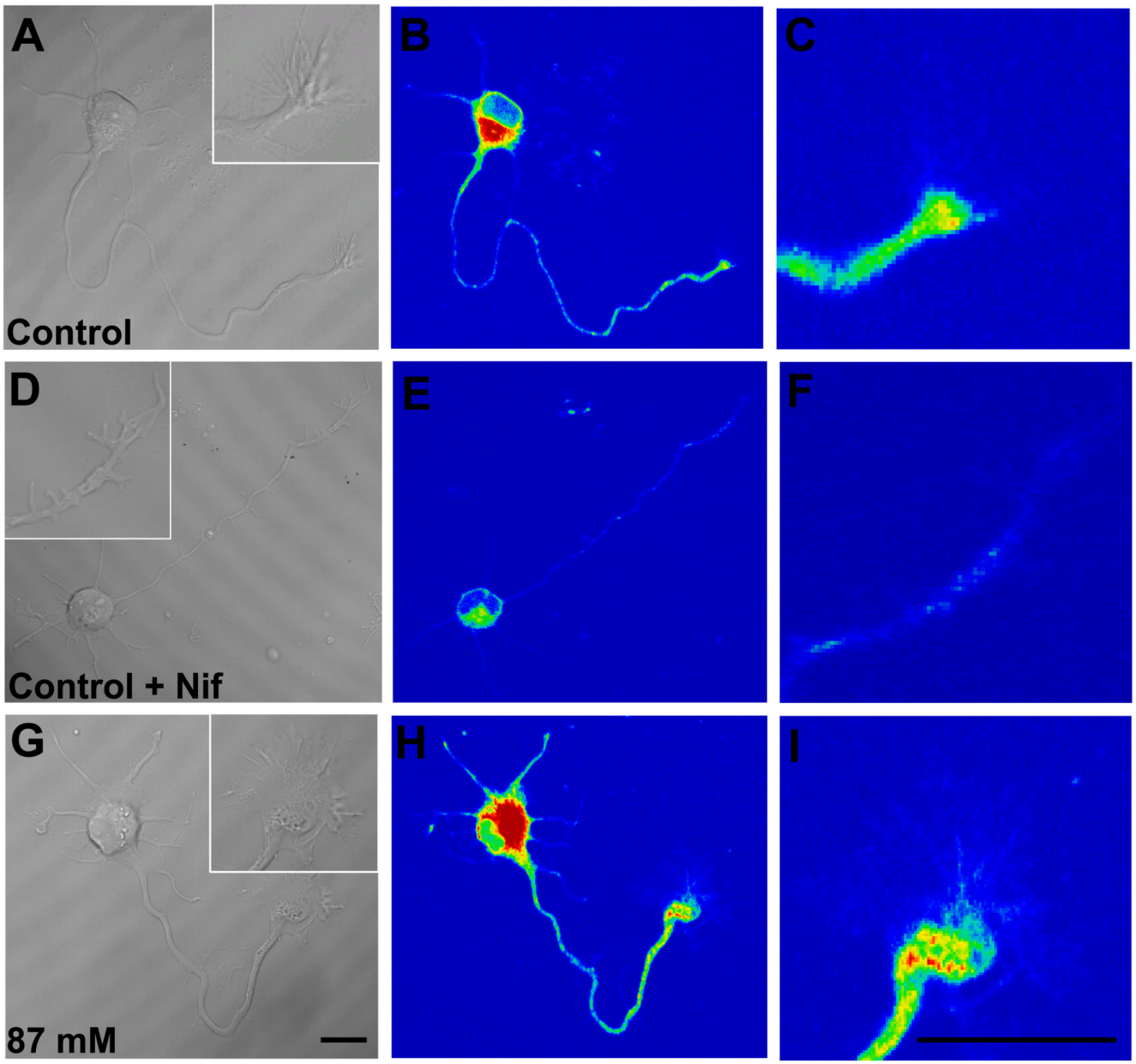

Figure 8. Visualization of L-type VDCCs in axonal growth cones by DM-Bodipy-DHP

Representative DIC and pseudocolor confocal images of DM-Bodipy-DHP fluorescence of Stage 3 hippocampal neurons maintained in control medium for 24 h after plating, then loaded with 100 μM of DM-Bodipy-DHP dye alone (*A–C*) or with dye and 10 μM nifedipine (D-F). *Insets* show the axonal growth cones at higher magnification. Nifedipine markedly reduced fluorescence intensity. Representative images of a hippocampal neuron maintained in medium containing 87 mM ethanol for 24 h after plating (G–I). Ethanol markedly increased fluorescence intensity in the soma, distal axon and axonal growth cone. Scale bar = 10 μm

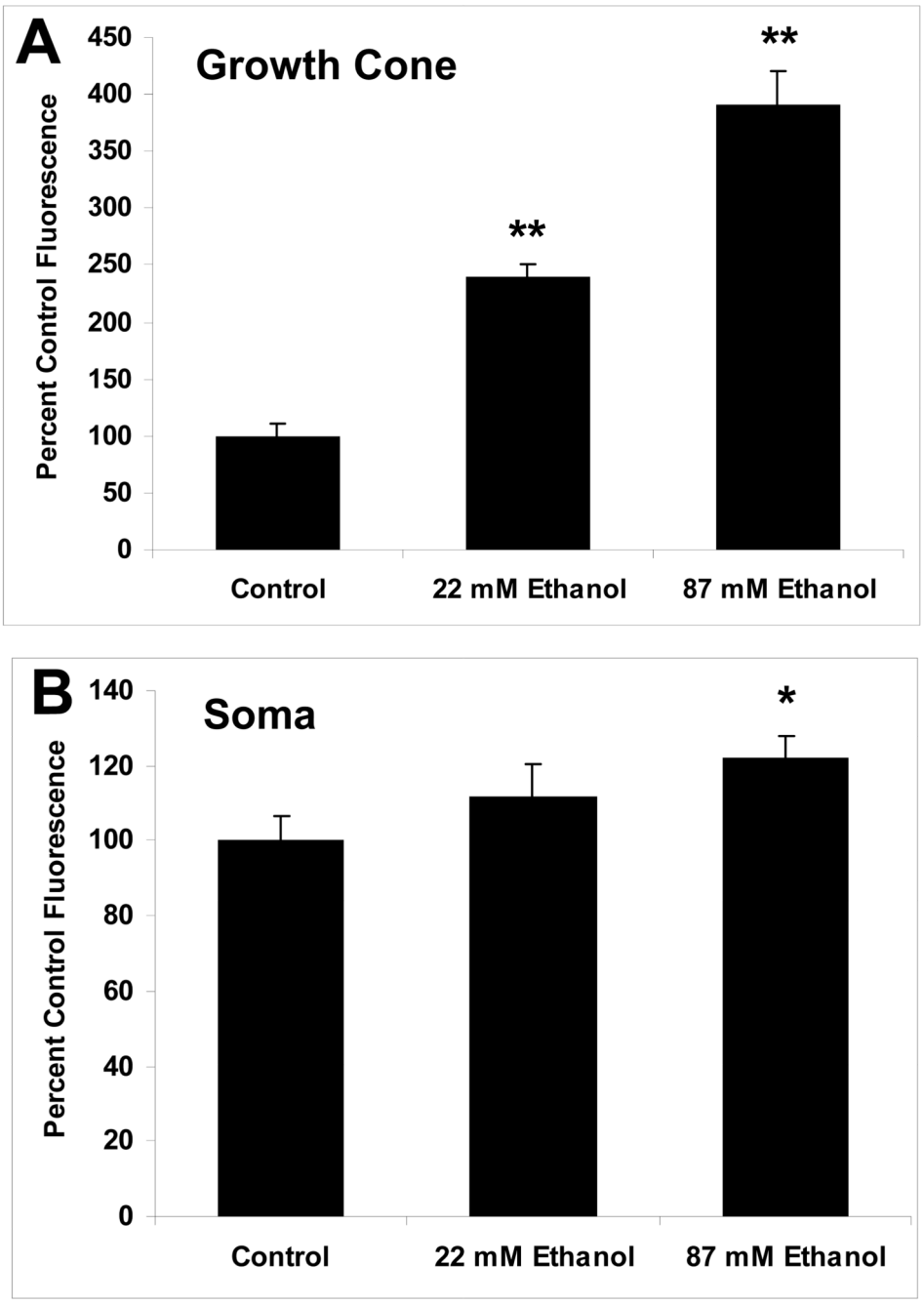

Figure 9. Summary plots of ethanol effects on DM-Bodipy-DHP fluorescence

Plots show fluorescence intensity in the axonal growth cones (*A*) and soma (*B*) of control and ethanol-exposed neurons. Data are the mean ± SEM for 18–33 growth cones in each treatment group in 2 separate cultures, expressed as percent of mean control fluorescence. ** $p < 0.0005$; * $p < .05$, compared to control (ANOVA with Newman-Keuls post hoc test).